Manuscript Number: egusphere-2024-2749

Dissipation ratio and eddy diffusivity of turbulent and salt finger mixing derived from microstructure measurements

Note: The reviewers' original comments are in black, and our responses are in blue.

Responses to Reviewer #1

There is a way of using the microstructure observations while recognizing that they are the sum of contributions from both (1) isotropic turbulence and (2) salt fingering. This method appeared in section 3 of McDougall and Ruddick (1992), and it is quite different to what is used in the present manuscript.

Reference:

McDougall, T. J. and B. R. Ruddick, 1992: The use of ocean microstructure to quantify both turbulent mixing and salt-fingering. Deep-Sea Research, 39, 1931-1952.

Responses: As suggested by the editor, here we add the comparison of the methods used in our manuscript with those described in McDougall and Ruddick (1992).

In the revised manuscript, we examined the "total" eddy diffusivities, K_θ and K_s, induced by superposed salt finger and turbulence by two different methods. The first is from McDougall and Ruddick (1992) (hereinafter MR92). MR92 does not need to differentiate salt finger and turbulent patches; it estimates the total eddy diffusivities by (i) evaluating the departure of observed Γ ($\Gamma = \frac{\chi_\theta N^2}{2\varepsilon\theta_z^2}$) from a preset reasonable turbulent Γ^T (e.g., Γ^T=0.265) and (ii) introducing a "salt flux enhancement factor", M_0, scaled by density ratio R_ρ and buoyancy flux ratio r (more details are given in McDougall and Ruddick (1992)). Here, r is treated specifically depending on the mixing type, that is, r^T=R_ρ for turbulence and r^F=$\frac{R_\rho\Gamma}{R_\rho\Gamma+R_\rho-1}$ for salt finger (St. Laurent and Schmitt, 1999).The second is from St. Laurent and Schmitt (1999) (hereinafter LS99), which differentiates turbulence and salt finger firstly, then estimates their eddy diffusivities separately, and finally obtains the total ones as K_θ = $P^T\cdot K_\theta^T$ + $P^F\cdot K_\theta^F$ and K_s = $P^T\cdot K_s^T$ + $P^F\cdot K_s^F$, where P^T and P^F are the number proportions of turbulence and salt finger patches to their sum, respectively. The methods used in our original manuscript is similar to LS99, except that we focus on the differences between salt finger and turbulence, and hence we did not estimate the "total" eddy diffusivities contributed jointly by salt finger and turbulence.

Fig. R1 shows the "total" K_θ estimated by above two methods for the five projects. Compared with the BBTREs and NATRE, the results based on MR92 and LS99 present larger differences for MIXETs, which may be due to the fewer patches and more scattered Γ^T and Γ^F for MIXETs. Nonetheless, it is obvious that both estimates have similar magnitude and vertical trend for all the five projects. This suggests that both MR92 and LS99 can reasonably estimate the total eddy diffusivities when sat finger and turbulence coexist. Because the method used to estimate diffusivities in our manuscript is essentially the same as LS99, the consistency between LS99 and MR92 adds to our confidence in the conclusions reached in this study.

Comparing the total K_θ with K_θ^T and K_θ^F (Figs 13, 14 in the manuscript, presented here as Figs. R2, R3), we can see K_θ, especially for the LS99 result, is obviously closer to K_θ^T for all the five projects, confirming that turbulence dominates the observed microstructures. This result addresses the reviewer's comment regarding "it is not appropriate to assume that salt fingers account for all the observed microstructure, as the present manuscript assumes" more thoroughly. We do note that K_θ in the upper 500 m for the BBTREs and NATRE are significantly lower than K_θ^T, seemingly indicating a strong weakening of K_θ due to the prevalence of salt finger. However, the effect of salt finger is actually overestimated, since the dominant hybrid mixing patches at this depth range are all excluded, which should be dominated by turbulence, as indicated by the elevated Re_b. Therefore, the total K_θ should not be so weak in the upper 500 m for the BBTREs and NATRE, and should be much closer to K_θ^T if the hybrid mixing patches enter the analysis.

Clearly, the total K_s is very similar to the situation of K_θ (Fig. R4), and the only notable difference is that K_s is not significantly weakened by salt finger in the upper 500 m for BBTREs and NATRE, owing to K_s^F is clearly greater than K_θ^F and is much closer to K_s^T.

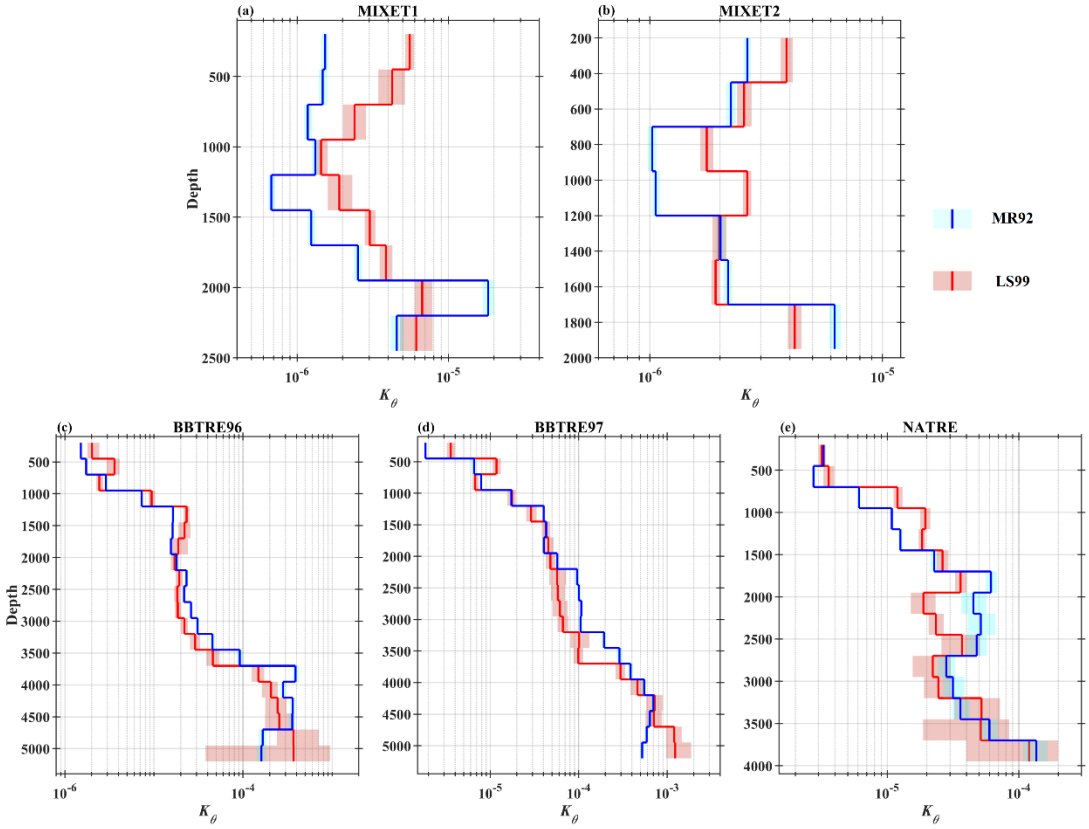

Fig. R1. Vertical profiles of depth-bin averaged total K_θ based on turbulence and salt finger patches for the five projects. The blue curves are results based on MR92, and the red ones are based on LS99. The shades correspond to 95% bootstrapped confidence intervals. The depth-bin size is 250 m, and depth bins with number of patches smaller than 10 are excluded.

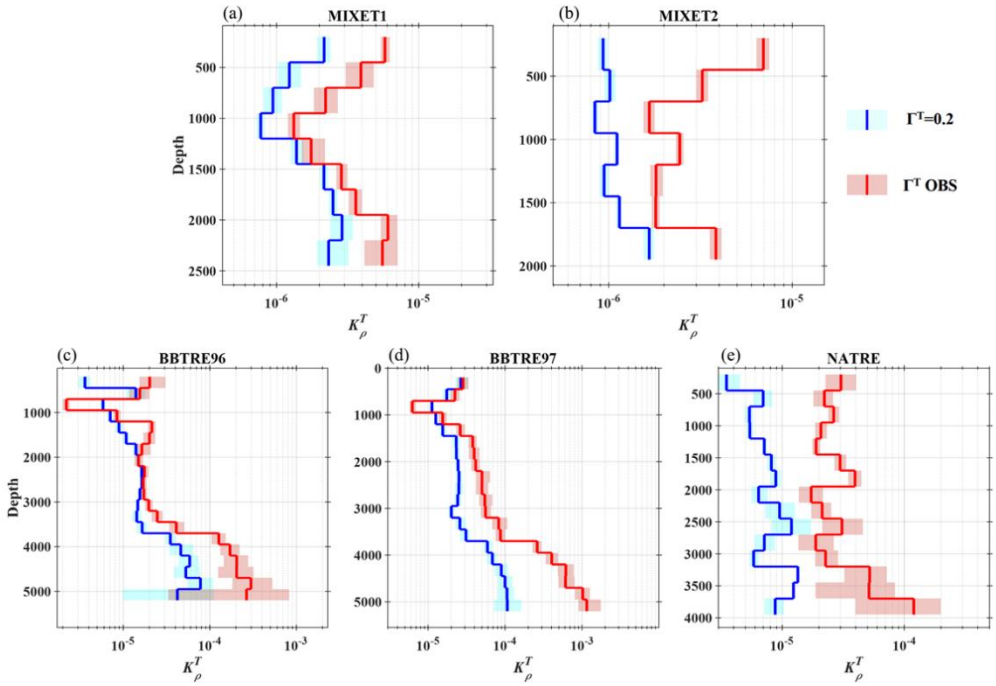

Fig. R2. Vertical profiles of depth-bin mean $K_\rho{}^T(K_c)$ based on energetic turbulence and weak turbulence patches for the five projects. The blue curve is K_c estimates by using Γ^T=0.2, and the red curve is $K_\rho{}^T$ based on the measured Γ^T. The shadings correspond to 95% bootstrapped confidence intervals. To exclude the influence of extreme values, we only consider patches with Γ^T within its upper and lower quartiles for each depth bin. The depth-bin size is 250 m.

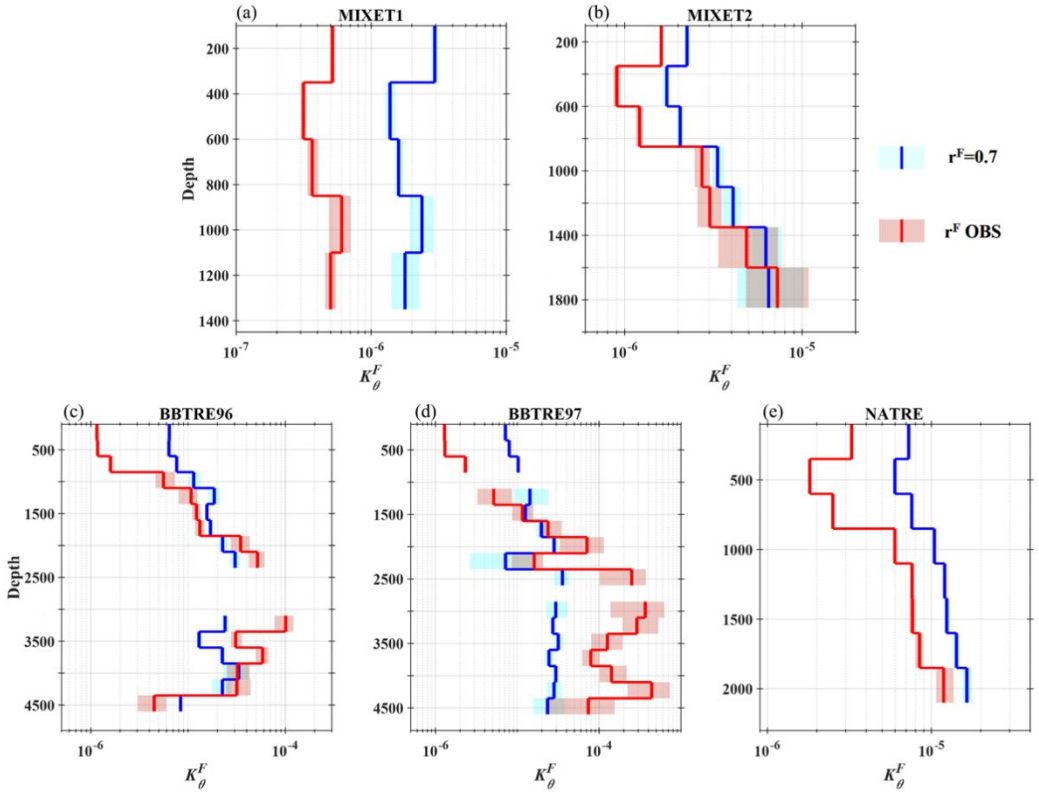

Fig. R3. Vertical profiles of depth-bin mean $K_\theta{}^F(K_\theta{}^F{}_c)$ based on salt finger patches for the five projects. The blue curves are $K_\theta{}^F{}_c$ estimated with r^F=0.7, and the red ones are $K_\theta{}^F$ based on the measured r^F. The shades correspond to 95% bootstrapped confidence intervals. To exclude the influence of extreme values, we only use patches with $\Gamma_\theta{}^F$ between its upper and lower quartiles for each depth bin. The depth-bin size is 250 m, and depth bins with number of patches smaller than 10 are excluded.

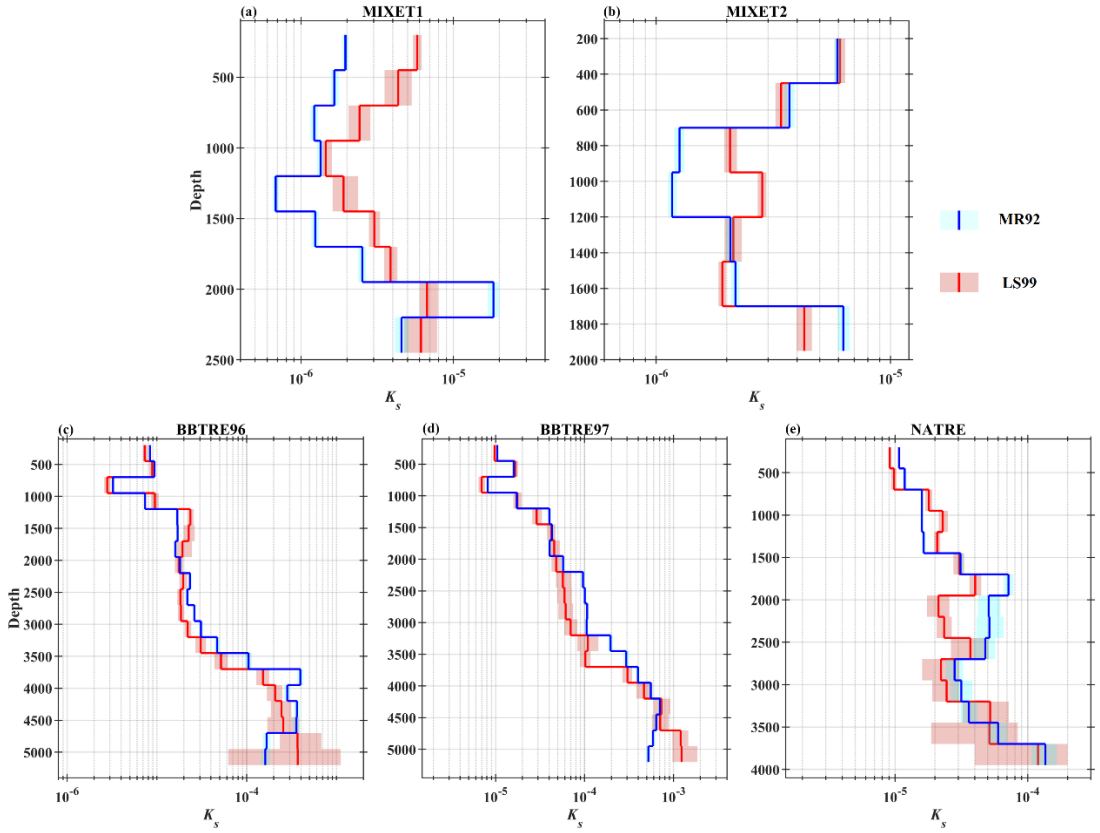

Fig. R4. Same as Fig. R1, but for the total K_S.

The main results presented above has been organized as a new subsection (Section 5.3) in the revised manuscript as following. We hope this revision could satisfy the reviewer.

"5.3 "Total" eddy diffusivities under superposed salt finger and turbulence

We examine the "total" eddy diffusivities contributed by both salt finger and turbulence by combining the patches with weak turbulence, energetic turbulence and salt finger. Two different methods are used to estimate the "total" eddy diffusivities. The first is from McDougall and Ruddick (1992) (hereinafter MR92). MR92 does not need to differentiate salt finger and turbulent patches; it estimates the total eddy diffusivities by (i) evaluating the departure of observed Γ (Eq. (1)) to a preset reasonable turbulent Γ^T (e.g., Γ^T=0.265) and (ii) introducing a "salt flux enhancement factor", M_0, scaled by R_ρ and r (more details are given in McDougall and Ruddick (1992)). Here, r is treated specifically depending on the mixing type, that is, r^T=R_ρ for turbulence and r^F=$\frac{R_\rho\Gamma}{R_\rho\Gamma+R_\rho-1}$ for salt finger (St. Laurent and Schmitt, 1999). The second is from St. Laurent and Schmitt (1999) (hereinafter LS99), which differentiates turbulence and salt finger firstly, then estimates their eddy diffusivities separately, and finally obtains the total ones as K_θ = $P^T \cdot K_\theta^T$ + $P^F \cdot K_\theta^F$ and K_s = $P^T \cdot K_s^T$ + $P^F \cdot K_s^F$, where P^T and P^F are the number proportions of turbulence and salt finger patches to their sum, respectively. Fig. 17 shows the "total" K_θ estimated by these two methods. Compared with the BBTREs and NATRE, the results based on MR92 and LS99 present larger differences for MIXETs, which may be due to the fewer patches and more scattered Γ^T and Γ^F. Nonetheless, it is obvious that both estimates have similar magnitude and vertical trend for all the five projects. Comparing the total K_θ with K_θ^T and K_θ^F (Figs. 13, 14), we can see K_θ, especially for the LS99 result, is obviously closer to K_θ^T for all the five projects, confirming that turbulence dominates the observed microstructures. Note that K_θ in the upper 500 m for the BBTREs and NATRE are significantly lower than K_θ^T, seemingly indicating a strong weakening of K_θ due to the prevalence of salt finger. However, the effect of salt finger is actually overestimated, since the dominant hybrid mixing patches at this depth range are all excluded, which should be dominated by turbulence, as indicated by the elevated Re_b. The total K_s is not shown since it is very similar to the situation of K_θ, and the only notable difference is K_s is not significantly weakened by salt finger in the upper 500 m for BBTREs and NATRE, owing to K_s^F is clearly greater than K_θ^F and much closer to K_s^T (Fig. 15).

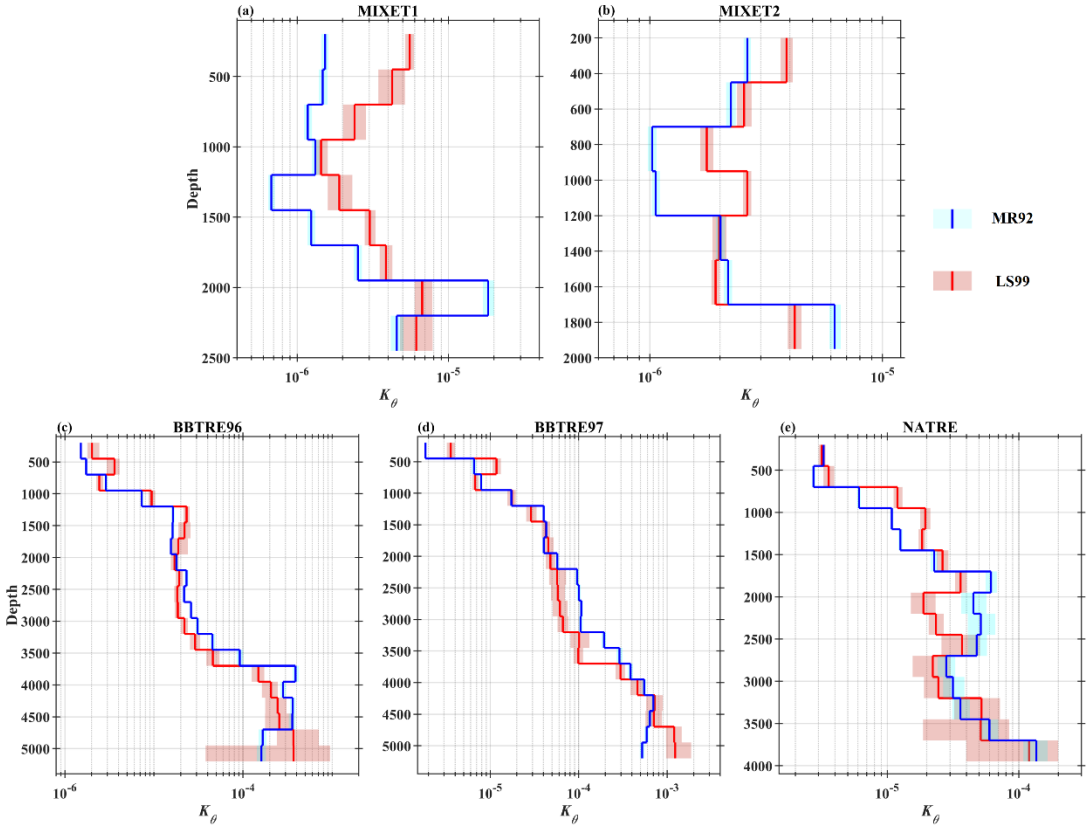

Fig. 17. Vertical profiles of depth-bin averaged total K_θ based on turbulence and salt finger patches for the five projects. The blue curves are results based on MR92, and the red ones are based on LS99. The shades correspond to 95% bootstrapped confidence intervals. The depth-bin size is 250 m, and depth bins with number of patches smaller than 10 are excluded."

Reference:

McDougall, T. J., and B. R. Ruddick, 1992: The use of ocean microstructure to quantify both turbulent mixing and salt-fingering. Deep Sea Research Part A. Oceanographic Research Papers, 39, 1931–1952, https://doi.org/10.1016/0198-0149(92)90006-F.

St. Laurent, L., and R. W. Schmitt, 1999: The contribution of salt fingers to vertical mixing in the North Atlantic Tracer Release Experiment. Journal of Physical Oceanography, 29, 1404–1424, https://doi.org/10.1175/1520-0485(1999)029<1404:tcosft>2.0.co;2.